Fluorescence

DOI: 10.1002/anie.201200853

Triple-Color Super-Resolution Imaging of Live Cells: Resolving Submicroscopic Receptor Organization in the Plasma Membrane**

*Stephan Wilmes, Markus Staufenbiel, Domenik Liße, Christian P. Richter, Oliver Beutel, Karin B. Busch, Samuel T. Hess, and Jacob Piehler**

The spatiotemporal organization of receptor proteins into submicroscopic structures in the plasma membrane is believed to play a critical role in regulation and coordination of signaling pathways. Several specific features of the plasma membrane have been shown to contribute to the transient assembly of nanoscopic heterogeneities (20–200 nm).[1] Fluorescence imaging techniques based on single-molecule localization provide versatile means for probing such submicroscopic organization of the cell with a resolution beyond the diffraction limit.[2] Super-resolution (SR) imaging in living cells is possible by fluorescence photoactivation localization microscopy (FPALM), for which various photoactivatable and photoswitchable autofluorescent proteins have been employed successfully.[3] Multicolor FPALM imaging, however, is currently limited by the choice of photoactivatable proteins having sufficient brightness for single-molecule localization techniques. Successful combination of photoactivatable green fluorescent protein (PAGFP) with photoactivatable orange fluorescent proteins such as PAmCherry[3c] or PAtagRFP[3e] has been reported. Triple-color FPALM imaging by including PAmKate is possible but limited by its significant spectral overlap with PAmCherry.[4] Herein we aimed to overcome this limitation by combination of dual-color FPALM with direct stochastic optical reconstruction microscopy (dSTORM).[5] This technique is based on photochemically trapping fluorophores in the dark state under reducing conditions, and can be applied to numerous fluorophores.[6] For the red fluorescent dye ATTO655, which is particularly susceptible to photoreduction, efficient photoswitching in the cytoplasm of living cells has been demonstrated.[5b,6b,7] This dye could be ideal for the combination with FPALM imaging using green and orange fluorescent photoactivatable proteins. A key challenge for its application in live-cell imaging, however, is the specific labeling of target proteins in the cytoplasm with ATTO655. Recently, a live-cell labeling approach based on a noncovalent interaction has been successfully demonstrated.[7] For more robust, long-term fluorescence labeling, however, irreversible attachment of the dye to the target proteins is preferable.

To readily combine dSTORM with dual-color FPALM, we aimed for implementing fast and efficient covalent labeling of the target proteins inside the cells with ATTO655. To this end, we have employed covalent labeling by means of the HaloTag, which has been reported to react rapidly with its substrate.[8] Moreover, the relatively hydro-

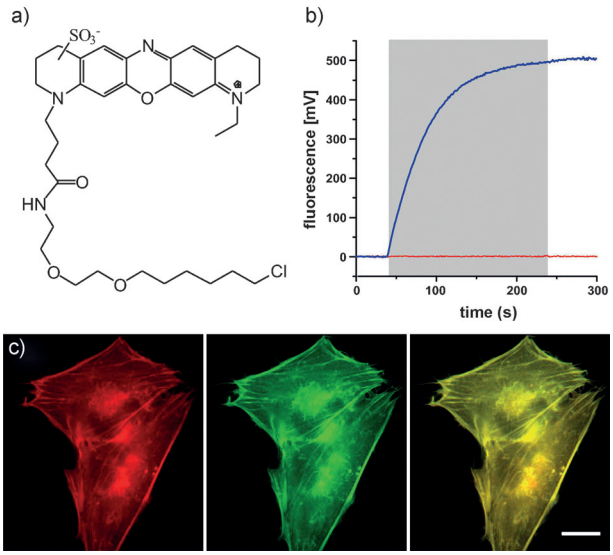

Figure 1. Efficient and specific covalent labeling with HTL–ATTO655. a) Structure of HTL–ATTO655. b) Reaction of 100 nM HTL–ATTO655 with immobilized HaloTag as detected by TIRFS (blue line). As a negative control, binding of HTL–ATTO655 to a blank surface was probed (red line). The injection period is marked in grey. c) Epifluorescent image of HeLa cells stably transfected with Lifeact–EGFP–HaloTag after incubation with HTL–ATTO655. Green: GFP channel; red: ATTO655 channel; yellow: overlay (scale bar: 20 μm).

[*] S. Wilmes,[+] M. Staufenbiel,[+] D. Liße, C. P. Richter, O. Beutel, Prof. Dr. J. Piehler
Division of Biophysics, Department of Biology
University of Osnabrück
Barbarastr. 11, 49076 Osnabrück (Germany)
E-mail: piehler@uos.de
Homepage: http://www.biologie.uni-osnabrueck.de/Biophysik/Piehler/

Prof. Dr. K. B. Busch
Mitochondrial Dynamics, Department of Biology
University of Osnabrück (Germany)

Prof. Dr. S. T. Hess
Department of Physics and Astronomy and Institute for Molecular Biophysics, University of Maine, ME (USA)

[+] These authors contributed equally to this work.

[**] We thank Gabriele Hikade and Hella Kenneweg for technical support, Roland Wedlich-Söldner (MPI Martinsried) for providing a plasmid coding for Lifeact, Volker Haucke (Freie Universität Berlin) for providing a plasmid coding for clathrin light chain, and Vladislav Verkhusha (Albert Einstein College of Medicine, New York) for a plasmid coding for PAtagRFP. This project was supported by funding from the DFG (PI405-5 and SFB 944), the European Community's Seventh Framework Programme (FP7/2007-2013) under grant agreement number 223608 (IFNaction), and the National Institute of General Medical Sciences (GM094713).

Supporting information for this article is available on the WWW under http://dx.doi.org/10.1002/anie.201200853.

phobic nature of the HaloTag ligand (HTL; Figure 1a) may better support efficient permeation of the substrate across the plasma membrane compared to other labeling techniques. This is particularly important because the zwitterionic nature of ATTO655 impedes its membrane permeability. ATTO655 was coupled to the HTL by *N*-hydroxy succinimidyl chemistry (see Scheme S1 in the Supporting Information) and efficient reaction with the HaloTag was confirmed in vitro by solid-phase binding assays based on simultaneous total internal reflection fluorescence spectroscopy (TIRFS) and reflectance interference (RIf) detection.[9] For this purpose, purified HaloTag was immobilized through its His-tag (see Figure S1 in the Supporting Information) and binding of HTL–ATTO655 was monitored in real time by TIRFS (Figure 1b). Specific and very rapid binding was detected, thus yielding a reaction rate constant of $(8\pm3)\times10^5\,\text{M}^{-1}\,\text{s}^{-1}$. Surprisingly, an HTL derivative with a longer ethylene glycol linker showed a 10-fold slower rate constant (Figure S1c). For this reason, we used compound **1** for further labeling experiments.

Protein labeling in living cells was explored by using HeLa cells stably expressing Lifeact fused to both monomeric enhanced green fluorescent protein (mEGFP) and the HaloTag (Lifeact–EGFP–HaloTag). Lifeact specifically binds to actin and therefore can be used for labeling the actin cytoskeleton in living cells,[10] and has been already exploited for SR imaging.[11] After incubating these cells with HTL–ATTO655, efficient labeling of the cytoskeleton was confirmed by epifluorescence microscopy (Figure 1c). A very good correlation of the EGFP and the ATTO655 channel can be seen. Moreover, no increase in the background for the ATTO655 channel compared to the GFP channel was observed, thus confirming the efficient washout of excess HTL–ATTO655. These results demonstrate successful permeation of HTL-ATTO655 across the membrane and specific reaction with the HaloTag in the cellular context. Thus, efficient and selective labeling of the HaloTag within the cytosol was achieved with HTL–ATTO655.

In the next step, we employed this labeling technique for SR imaging of the actin cytoskeleton in live cells by dSTORM. To selectively image the membrane cytoskeleton, total internal reflection fluorescence microscopy (TIRFM) was applied. Upon illumination of these cells with increased laser power (ca. 0.2–0.4 $\text{kW}\,\text{cm}^{-2}$), rapid decay of the fluorescence intensity was observed until a steady state was reached and blinking of individual ATTO655 molecules could be discerned. The decay of the particle localization density of fluorescent ATTO655 could be substantially slowed by pulsed illumination at $\lambda = 405$ nm (see Figure S2 in the Supporting Information).[5b] Under these conditions, a relatively moderate decrease of localizations/frame from 0.20 molecules μm^{-2} to 0.05 molecules μm^{-2} was detected within 10000 frames with an average localization precision of 20–25 nm (Figure S3). Live-cell SR images of the membrane skeleton obtained from these measurements by single-molecule localization are shown in Figure 2. Compared to the diffraction-limited image, a much higher resolution was obtained (Figure 2b,c and Figure S3) and submicroscopic filaments with diameters below 100 nm could be discerned (Figure 2d and e).

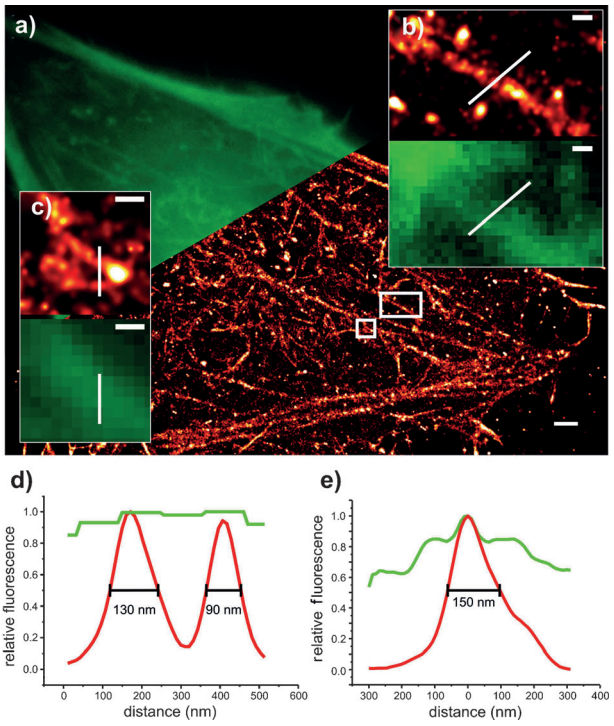

Figure 2. Live-cell SR imaging with HTL–ATTO655. a) Live HeLa cells stably transfected with Lifeact–EGFP–HaloTag after staining with HTL–ATTO655 as detected on the GFP channel (green) compared to an SR image rendered from individual ATTO655 molecules. Imaging was carried out by continuous excitation at $\lambda = 647$ nm with a readout time of 32 ms/frame (scale bar: 2 μm). b,c) Detailed images of the boxed regions showing the diffraction-limited GFP channel (green) and SR image obtained from dSTORM imaging (red hot; scale bar: 300 nm). d,e) Cross-sections through actin filaments shown in panels c and b, respectively (Super-resolved: red line; diffraction-limited: green line). The full-width at half-maximum is shown in nanometers.

Reversible photoswitching of the dye in combination with the reversible binding of Lifeact to the cytoskeleton enabled imaging over extended time periods (typically 10000 frames). By rendering images from substacks of 1000 frames, time-lapse SR images were obtained, thus enabling the dynamics of the membrane skeleton to be resolved on the nanoscale level (Figure 3a and see Video 2 in the Supporting Information).

Having established site-specific cytosolic labeling with ATTO655 and SR imaging of cellular structures by dSTORM, we explored imaging of more dynamic cellular nanostructures at the plasma membrane. We chose clathrin-coated pits, which play an important role in regulating cell signaling and have been shown to be involved in the endocytosis of the type I interferon receptor (IFNAR) signaling complex.[12] For SR imaging of clathrin-coated pits, clathrin light chain (CLC) fused to the HaloTag (CLC–HaloTag) was expressed and labeled in the cell with HTL–ATTO655 as described above. Upon imaging CLC–HaloTag/ATTO655, bound to the cytosolic leaflet of the plasma membrane, by excitation in TIRF mode, fluctuations of signals from individual ATTO655 molecules were observed over extended time periods with high localization precision (see Video 3 and Figure S4 in the Supporting Information). A cumulative SR image rendered

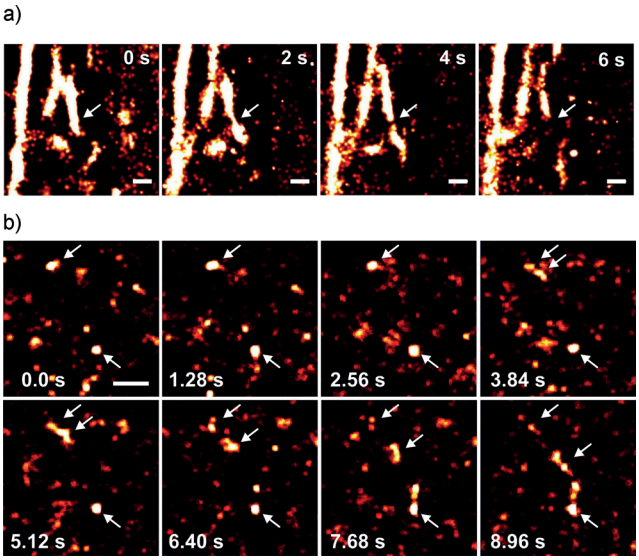

Figure 3. Time-lapse SR imaging of cellular nanostructures. a) Dynamics of the cortical actin skeleton stained with Lifeact–HaloTag/ATTO655. Each image was rendered 1000 frames (scale bar: 500 nm). b) SR dynamics of clathrin-coated pits at the plasma membrane stained with CLC–HaloTag/ATTO655. Each image was rendered from 50 frames (scale bar: 1 μm).

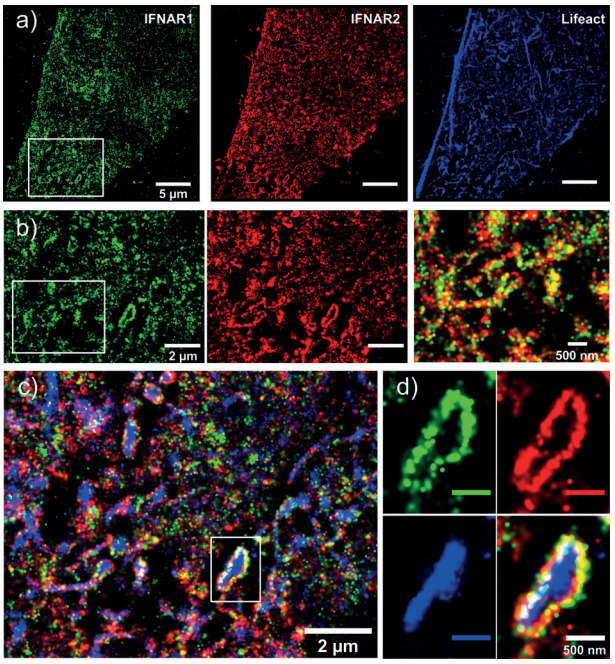

Figure 4. Simultaneous triple-color SR imaging in live cells. HeLa cells transiently transfected with IFNAR1-PAGFP (green), IFNAR2–PAtagRFP (red) and Lifeact–HaloTag labeled with HTL–ATTO655 (blue). Imaging was carried out in cycles starting with photoactivation at $\lambda = 405$ nm (4 ms) followed by sequential readout during excitation at $\lambda = 488$, 568, and 647 nm (32 ms each), respectively. SR images were obtained from 1000 frames taken within 90 s. a) SR images obtained from the three channels. b) Detailed close-up of a region of interest (ROI) in the image for IFNAR1 and IFNAR2 marked in (a) and an overlay of the two channels. c) Overlay of IFNAR1, IFNAR2, and the cytoskeleton in the same ROI. d) Enlarged ROI showing the cytoskeletal association of IFNAR1 and IFNAR2 (scale bar: 500 nm).

from 1000 frames is shown in Figure S5 in the Supporting Information. However, clathrin nanostructures could be discerned in images rendered from only 50 frames. Therefore, time-lapse SR image sequences were assembled by rendering 50 frames (1.28 s) with a step size of 10 frames (Figure 3b and Video 4). These time-lapse SR image sequences revealed rapid nanoscale dynamics of clathrin structures. Thus, directed motion of clathrin-coated vesicles, probably resulting from endocytosis events, could be observed with a resolution of approximately 30 nm. From these time-lapse experiments, a transport velocity of about 400 nm s^{-1} was estimated, which is in good agreement with previous studies.[13]

Having established live-cell dSTORM microscopy based on labeling with ATTO655, we tested the combination with dual-color FPALM. To this end, we transiently co-expressed the subunits of the type I interferon receptor, IFNAR1 and IFNAR2 fused to PAGFP and PAtagRFP, respectively. Dual-color FPALM imaging in TIRF mode yielded SR images demonstrating heterogeneous distribution of both receptor subunits in the plasma membrane (Figures 4a,b). Strikingly, partial co-clustering of both receptor subunits in submicroscopic domains was observed. To identify the cellular nanostructures underlying these clusters, CLC–HaloTag or Lifeact–HaloTag were transiently co-expressed with IFNAR1–PAGFP and IFNAR2–PAtagRFP. After staining with HTL–ATTO655, images were acquired by repeated cycles of photoactivation at $\lambda = 405$ nm and sequential excitation at $\lambda = 488$, 568, and 647 nm (each 32 ms), thus yielding triple-color SR images with a cycle interval time of approximately 155 ms (see Figure S6 in the Supporting Information). Only weak co-localization of IFNAR1 and IFNAR2 with CLC could be observed (see Figure S7 in the Supporting Information). In contrast, SR images of IFNAR1 and IFNAR2 in combination with Lifeact–HaloTag revealed nanostructured co-organization of the receptor subunits at the membrane skeleton (Figure 4c and Figure S8). Remarkably, IFNAR1 and IFNAR2 were frequently found in the periphery of actin structures (Figure 4d), thus suggesting interaction with actin or actin-bound adaptor proteins. Indeed, several adaptor and scaffolding proteins have been suggested to play a key role for IFN signaling.[14] Moreover, cytoskeletal association has previously been suggested to be involved in type I IFN receptor activation.[15] Further experiments will be required to characterize these interactions at the membrane skeleton in more detail.

In summary, we have here established triple-color SR imaging in living cells by combination of dSTORM and FPALM. While several approaches for multicolor SR imaging in fixed cells have been reported,[3d,16] triple-color imaging under physiological conditions remains challenging.[4] HaloTag-specific labeling with HTL–ATTO655 allows efficient, irreversible labeling of fusion proteins in the cytoplasm of living cells, which makes it advantageous compared to previously reported, noncovalent labeling. Since ATTO655 is not readily membrane permeable, conjugation to the hydrophobic HTL may contribute to the good labeling efficacy. Moreover, labeling through the HaloTag is orthogonal to other posttranslational labeling techniques such as the

SNAP-tag and thus readily allows combination with other live-cell dSTORM dyes such as tetramethylrhodamine.[17] Based on this approach, we have demonstrated long-term SR imaging by dSTORM in living cells, which enables imaging the dynamics of cellular nanostructures over extended time periods. Imaging was possible under physiological conditions,[5b,6b,7] that is, without the need to add reducing agents into the supernatant as required for live-cell STORM.[18] The fluorescence emitted by ATTO655 can be spectrally well separated from the fluorescence emitted by orange fluorescent, photoactivatable proteins such as PAmCherry or PAtagRFP. Thus, dSTORM is readily combined with FPALM and simultaneous triple-color SR imaging was possible with an average localization precision of less than 25 nm in all channels (see Figure S9 in the Supporting Information). Based on this method, we were able to resolve characteristic submicroscopic co-organization of the subunits of a cytokine receptor in the context of the cytoskeleton. Combined dSTORM and FPALM will prove powerful for probing the dynamics of cellular microcompartments.

Received: January 31, 2012
Published online: April 5, 2012

Keywords: fluorescence · imaging agents · membrane proteins · protein–protein interactions · single-molecule studies

[1] a) D. Marguet, P. F. Lenne, H. Rigneault, H. T. He, *EMBO J.* **2006**, *25*, 3446 – 3457; b) A. Kusumi, Y. M. Shirai, I. Koyama-Honda, K. G. Suzuki, T. K. Fujiwara, *FEBS Lett.* **2010**, *584*, 1814; c) D. Lingwood, K. Simons, *Science* **2010**, *327*, 46 – 50.

[2] a) E. Betzig, G. H. Patterson, R. Sougrat, O. W. Lindwasser, S. Olenych, J. S. Bonifacino, M. W. Davidson, J. Lippincott-Schwartz, H. F. Hess, *Science* **2006**, *313*, 1642 – 1645; b) M. J. Rust, M. Bates, X. Zhuang, *Nat. Methods* **2006**, *3*, 793 – 795; c) J. Fölling, M. Bossi, H. Bock, R. Medda, C. A. Wurm, B. Hein, S. Jakobs, C. Eggeling, S. W. Hell, *Nat. Methods* **2008**, *5*, 943 – 945; d) G. Patterson, M. Davidson, S. Manley, J. Lippincott-Schwartz, *Annu. Rev. Phys. Chem.* **2010**, *61*, 345 – 367; e) T. Appelhans, C. P. Richter, V. Wilkens, S. T. Hess, J. Piehler, K. B. Busch, *Nano Lett.* **2012**, *12*, 610.

[3] a) S. T. Hess, T. P. Girirajan, M. D. Mason, *Biophys. J.* **2006**, *91*, 4258 – 4272; b) S. T. Hess, T. J. Gould, M. V. Gudheti, S. A. Maas, K. D. Mills, J. Zimmerberg, *Proc. Natl. Acad. Sci. USA* **2007**, *104*, 17370 – 17375; c) F. V. Subach, G. H. Patterson, S. Manley, J. M. Gillette, J. Lippincott-Schwartz, V. V. Verkhusha, *Nat. Methods* **2009**, *6*, 153 – 159; d) I. Testa, C. A. Wurm, R. Medda, E. Rothermel, C. von Middendorf, J. Folling, S. Jakobs, A. Schonle, S. W. Hell, C. Eggeling, *Biophys. J.* **2010**, *99*, 2686 – 2694; e) F. V. Subach, G. H. Patterson, M. Renz, J. Lippincott-Schwartz, V. V. Verkhusha, *J. Am. Chem. Soc.* **2010**, *132*, 6481.

[4] M. S. Gunewardene, F. V. Subach, T. J. Gould, G. P. Penoncello, M. V. Gudheti, V. V. Verkhusha, S. T. Hess, *Biophys. J.* **2011**, *101*, 1522 – 1528.

[5] a) J. Vogelsang, C. Steinhauer, C. Forthmann, I. H. Stein, B. Person-Skegro, T. Cordes, P. Tinnefeld, *ChemPhysChem* **2010**, *11*, 2475 – 2490; b) S. van de Linde, A. Loschberger, T. Klein, M. Heidbreder, S. Wolter, M. Heilemann, M. Sauer, *Nat. Protoc.* **2011**, *6*, 991 – 1009.

[6] a) S. van de Linde, U. Endesfelder, A. Mukherjee, M. Schuttpelz, G. Wiebusch, S. Wolter, M. Heilemann, M. Sauer, *Photochem. Photobiol. Sci.* **2009**, *8*, 465 – 469; b) M. Heilemann, S. van de Linde, A. Mukherjee, M. Sauer, *Angew. Chem.* **2009**, *121*, 7036 – 7041; *Angew. Chem. Int. Ed.* **2009**, *48*, 6903 – 6908.

[7] R. Wombacher, M. Heidbreder, S. van de Linde, M. P. Sheetz, M. Heilemann, V. W. Cornish, M. Sauer, *Nat. Methods* **2010**, *7*, 717 – 719.

[8] G. V. Los, L. P. Encell, M. G. McDougall, D. D. Hartzell, N. Karassina, C. Zimprich, M. G. Wood, R. Learish, R. F. Ohana, M. Urh, D. Simpson, J. Mendez, K. Zimmerman, P. Otto, G. Vidugiris, J. Zhu, A. Darzins, D. H. Klaubert, R. F. Bulleit, K. V. Wood, *ACS Chem. Biol.* **2008**, *3*, 373 – 382.

[9] M. Gavutis, S. Lata, J. Piehler, *Nat. Protoc.* **2006**, *1*, 2091 – 2103.

[10] J. Riedl, A. H. Crevenna, K. Kessenbrock, J. H. Yu, D. Neukirchen, M. Bista, F. Bradke, D. Jenne, T. A. Holak, Z. Werb, M. Sixt, R. Wedlich-Soldner, *Nat. Methods* **2008**, *5*, 605 – 607.

[11] I. Izeddin, C. G. Specht, M. Lelek, X. Darzacq, A. Triller, C. Zimmer, M. Dahan, *PLoS ONE* **2011**, *6*, e15611.

[12] M. Marchetti, M. N. Monier, A. Fradagrada, K. Mitchell, F. Baychelier, P. Eid, L. Johannes, C. Lamaze, *Mol. Biol. Cell* **2006**, *17*, 2896 – 2909.

[13] Y. Zhang, *Phys. Rev. E* **2011**, *83*, 011909.

[14] A. Usacheva, X. Tian, R. Sandoval, D. Salvi, D. Levy, O. R. Colamonici, *J. Immunol.* **2003**, *171*, 2989 – 2994.

[15] L. M. Pfeffer, N. Stebbing, D. B. Donner, *Proc. Natl. Acad. Sci. USA* **1987**, *84*, 3249 – 3253.

[16] a) M. Bossi, J. Folling, V. N. Belov, V. P. Boyarskiy, R. Medda, A. Egner, C. Eggeling, A. Schonle, S. W. Hell, *Nano Lett.* **2008**, *8*, 2463 – 2468; b) M. Bates, G. T. Dempsey, K. H. Chen, X. Zhuang, *ChemPhysChem* **2012**, *13*, 99 – 107; c) U. Endesfelder, S. Malkusch, B. Flottmann, J. Mondry, P. Liguzinski, P. J. Verveer, M. Heilemann, *Molecules* **2011**, *16*, 3106 – 3118.

[17] T. Klein, A. Loschberger, S. Proppert, S. Wolter, S. van de Linde, M. Sauer, *Nat. Methods* **2011**, *8*, 7 – 9.

[18] S. A. Jones, S. H. Shim, J. He, X. Zhuang, *Nat. Methods* **2011**, *8*, 499.

